Mono-InternVL: Pushing the Boundaries of Monolithic Multimodal Large Language Models with Endogenous Visual Pre-training

Gen Luo[1*], **Xue Yang**[1*], **Wenhan Dou**[2*], **Zhaokai Wang**[3,1*]
Jifeng Dai[2,1], **Yu Qiao**[1], **Xizhou Zhu**[2,1✉]
[1]OpenGVLab, Shanghai AI Laboratory   [2]Tsinghua University
[3]Shanghai Jiao Tong University

Project Page: Mono-InternVL

Abstract

The rapid advancement of Large Language Models (LLMs) has led to an influx of efforts to extend their capabilities to multimodal tasks. Among them, growing attention has been focused on monolithic Multimodal Large Language Models (MLLMs) that integrate visual encoding and language decoding into a single LLM. Despite the structural simplicity and deployment-friendliness, training a monolithic MLLM with promising performance still remains challenging. In particular, the popular approaches adopt continuous pre-training to extend a pre-trained LLM to a monolithic MLLM, which suffers from catastrophic forgetting and leads to performance degeneration. In this paper, we aim to overcome this limitation from the perspective of delta tuning. Specifically, our core idea is to embed visual parameters into a pre-trained LLM, thereby incrementally learning visual knowledge from massive data via delta tuning, *i.e.,* freezing the LLM when optimizing the visual parameters. Based on this principle, we present Mono-InternVL, a novel monolithic MLLM that seamlessly integrates a set of visual experts via a multimodal mixture-of-experts structure. Moreover, we propose an innovative pre-training strategy to maximize the visual capability of Mono-InternVL, namely Endogenous Visual Pre-training (EViP). In particular, EViP is designed as a progressive learning process for visual experts, which aims to fully exploit the visual knowledge from noisy data to high-quality data. To validate our approach, we conduct extensive experiments on 16 benchmarks. Experimental results not only validate the superior performance of Mono-InternVL compared to the state-of-the-art MLLM on 6 multimodal benchmarks, *e.g.,* +113 points over InternVL-1.5 on OCRBench, but also confirm its better deployment efficiency, with first token latency reduced by up to 67%.

1 Introduction

In recent years, the rapid development of Large Language Models (LLMs) (OpenAI, 2023; Bai et al., 2023a; Cai et al., 2024) has spurred increasing efforts to extend their multimodal capabilities (Chen et al., 2023; Liu et al., 2023e). As shown in Fig. 1 (a), most existing Multimodal Large Language Models (MLLMs) adopt a modular architecture, where visual encoding and language decoding are processed separately. This is typically achieved by combining a pre-trained visual encoder like CLIP-ViT (Radford et al., 2021) with an LLM (Liu et al., 2023e; Chen et al., 2024c; Li et al., 2023a). Recent research has also started exploring monolithic MLLMs (Bavishi et al., 2023; Diao et al., 2024; Chen et al., 2024b), as shown in Fig. 1 (b), which integrate visual perception and multimodal understanding directly into a single LLM. Due to their simplicity and unity, monolithic MLLMs can be more easily deployed using existing LLM inference libraries (LMDeployContributors, 2023) and show superior efficiency than modular MLLMs (Diao et al., 2024; Chen et al., 2024b).

Despite recent progress, training a monolithic MLLM with promising performance still remains challenging. In particular, monolithic MLLMs struggle to replicate the successful usage of pre-
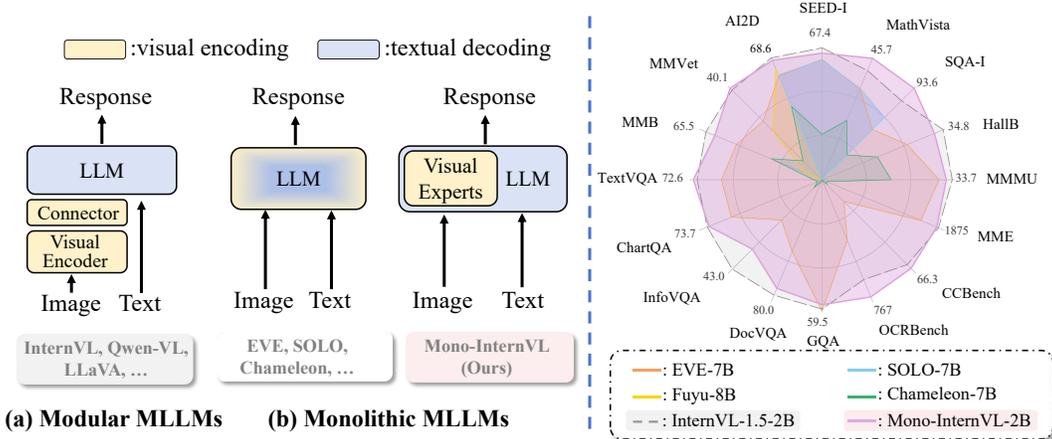

Figure 1: **Comparison of Mono-InternVL and existing MLLMs.** Compared with modular MLLMs, Mono-InternVL embeds visual experts into the pre-trained LLM and integrates visual encoding and language decoding into a single LLM. Through endogenous visual pre-training, Mono-InternVL significantly pushes the performance boundaries of monolithic MLLMs.

trained visual encoders in modular MLLMs for visual perception. Therefore, researchers often rely on additional pre-training to compensate for the shortcomings in visual perception in monolithic MLLMs (ChameleonTeam, 2024; Diao et al., 2024). A straightforward approach is the *native pre-training* (ChameleonTeam, 2024), which pre-trains a monolithic MLLM from scratch using a mixture of text-only and multimodal data. However, it requires prohibitively high training costs and often suffers from challenges of unstable optimization (ChameleonTeam, 2024). Another common solution is the *continuous pre-training* (Diao et al., 2024), which extends the pre-trained LLM to multimodality via additional visual pre-training. Benefiting from the knowledge in the pre-trained LLM, the cost of continuous pre-training becomes much more affordable. Nevertheless, due to the catastrophic forgetting issue (Zhai et al., 2023), the pre-trained language knowledge is inevitably undermined during continuous pre-training, thereby weakening the multimodal capabilities.

In this paper, we aim to address the forgetting issue of continuous pre-training through *delta tuning* (Ding et al., 2022). In particular, we argue that such issue arises from the shared architecture for joint vision and language modeling, where optimizations for vision can negatively impact language capabilities. Therefore, it is a natural thought to introduce an independent visual parameter set into the pre-trained LLM, which allows formulating visual pre-training with partial parameter tuning. This can help retain the language knowledge by freezing the entire LLM during continuous pre-training, while improving visual learning. This principle is also aligned with previous endeavors in modular MLLMs, *e.g.,* QwenVL (Bai et al., 2023b) and InternVL-1.5 (Chen et al., 2024c), where the visual parameters are placed outside the LLM.

Based on the above principle, we propose a novel monolithic MLLM, namely Mono-InternVL. As shown in Fig. 2, the visual parameters in Mono-InternVL are designed as a set of expert networks that are seamlessly integrated into the LLM via the mixture-of-experts mechanism. To better capture the visual knowledge, these experts are initialized from the Feed-Forward Networks (FFNs) in the pre-trained LLM. Based on this architecture, we present an innovative visual pre-training method called *Endogenous Visual Pre-training* (EViP). Specifically, EViP is formulated as a progressive learning process of three stages: 1) concept learning to grasp basic visual concepts, 2) semantic learning to capture high-level semantics, *e.g.,* world knowledge, and 3) alignment learning to align knowledge with downstream tasks. Benefiting from the architecture and the pre-training strategy, the visual scalability of Mono-InternVL is fully unleashed, where the downstream performance consistently improves as the scale of the pre-training data increases. After visual pre-training, Mono-InternVL accommodates complex multimodal tasks via supervised instruction tuning.

To validate our method, we develop Mono-InternVL using the pre-trained LLM InternLM2-1.8B (Cai et al., 2024), and conduct extensive experiments on 16 multimodal benchmarks. Experimental results not only demonstrate the significant performance improvements of Mono-InternVL

against previous monolithic MLLMs, but also validate its superior efficiency compared to existing modular MLLMs. For instance, Mono-InternVL with 1.8 billion activated parameters can outperform existing monolithic MLLMs with 7 billion parameters by a significant margin, *e.g.,* +15.5% over EVE on average. Compared to the state-of-the-art modular MLLM InternVL-1.5 (Chen et al., 2024c), Mono-InternVL shows superior performance on 6 multimodal benchmarks while reducing first token latency by 67%. In conclusion, our contributions can be summarized in threefold:

- We present Mono-InternVL, a novel monolithic MLLM that seamlessly integrates a set of visual experts via a multimodal mixture-of-experts architecture. This architecture can effectively extend the pre-trained LLM to a monolithic MLLM while retaining the pre-trained knowledge.

- We propose a novel visual pre-training approach for Mono-InternVL called endogenous visual pre-training (EViP). EViP adopts a progressive learning strategy to encourage visual experts of Mono-InternVL to continuously grasp visual knowledge from noisy data to high-quality data.

- Mono-InternVL demonstrates for the first time that the leading performance of MLLM no longer depends on the pre-trained visual encoder, thereby opening new avenues for designing future MLLMs. In particular, Mono-InternVL achieves the state-of-the-art (SoTA) results compared to existing MLLMs on 6 multimodal benchmarks.

2 RELATED WORK

Modular multimodal large language models. Recent progress in large language models (LLMs) has catalyzed the integration of vision and language modalities, giving rise to multimodal large language models (MLLMs). Both commercial entities, such as GPT-4V (Yang et al., 2023) and Gemini series (Team et al., 2023), and other open-source initiatives, *e.g.* BLIP series (Li et al., 2022; 2023a; Dai et al., 2023), LLaVA series (Liu et al., 2023e;d; 2024), InternVL (Chen et al., 2023; 2024c), have pursued this integration, often linking LLMs (Touvron et al., 2023a;b; Team, 2023; Cai et al., 2024) with large vision models (LVMs) (Radford et al., 2021; Dosovitskiy et al., 2021; Dehghani et al., 2023; Chen et al., 2023) via intermediate layers. Specifically, there are lightweight MLLMs (*i.e.,* $\leq$ 4B parameters), such as MobileVLM-V2 (Chu et al., 2024), Mini-Gemini (Li et al., 2024), MM1 (McKinzie et al., 2024), DeepSeek-VL (Lu et al., 2024), PaliGemma (Beyer et al., 2024) and MiniCPM-V (Yao et al., 2024). However, such encoder-based vision-language models (modular MLLMs) encounter challenges like limitations in input processing due to pre-trained visual encoders, deployment inefficiencies, and complexities in balancing the capacities of LLMs and LVMs, as also pointed out by (Diao et al., 2024).

Monolithic multimodal large language models. The issues related to modular MLLMs have steered research toward encoder-free architectures, also known as monolithic MLLMs, which can be summarized into two categories. The first category obtains continuous visual tokens through a lightweight structure before feeding into MLLMs. For instance, Fuyu-8B (Bavishi et al., 2023) processes images directly through a simple linear projection, adeptly handling high-resolution images without using a dedicated visual encoder. EVE-7B (Diao et al., 2024) prioritizes vision-language pre-alignment from an LLM-centric perspective and enhances image recognition through visual representation supervision. SOLO (Chen et al., 2024b) introduces an open-source training recipe for developing monolithic MLLMs. In contrast, the second category introduces VQ tokenizer-based models to generate discrete visual tokens to support image generation tasks, with representative works such as Chameleon (ChameleonTeam, 2024), Show-o (Xie et al., 2024), Transfusion (Zhou et al., 2024), and Emu3 (Wang et al., 2024b).

Multimodal mixture-of-experts. VLMo (Bao et al., 2022) and BEiT-3 (Wang et al., 2022) employ a pool of modality experts to replace the feed-forward network in standard Transformer to capture modality-specific information by switching to different modality experts, and use the shared self-attention across modalities to align visual and linguistic information. VL-MoE (Shen et al., 2023) introduces mixture-of-experts (MoE) (Yuksel et al., 2012) based on the above works for better training and deploying. MoMa (Lin et al., 2024) also uses multimodal mixture-of-experts for pre-training of MLLMs (ChameleonTeam, 2024) and cooperates with sparse components, *e.g.* MoE and mixture-of-depths (MoD) (Raposo et al., 2024) to improve the efficiency of pre-training from scratch with trillions of mixed-modal tokens. Inspired by the above literature, we introduce multimodal mixture-of-experts (*i.e.,* a visual expert and a language expert) for pre-training monolithic MLLMs and use
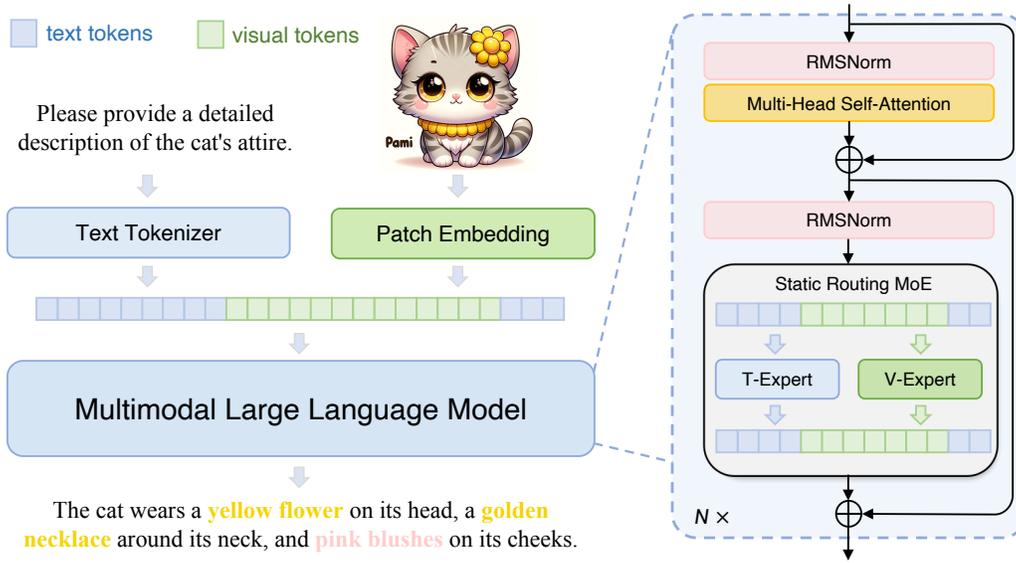
Figure 2: **Monolithic architecture of Mono-InternVL.** Mono-InternVL is designed as a multimodal MoE structure, where visual and textual tokens are processed by the corresponding experts. Such a design greatly facilitates the visual pre-training while retaining the model efficiency.

a novel progressive learning strategy, named endogenous visual pre-training (EViP), to address the unique challenges faced by monolithic MLLMs.

3 MONO-INTERNVL

3.1 THE MONOLITHIC ARCHITECTURE

As shown in Fig. 2, we first outline the architecture of Mono-InternVL, which consists of tokenizers and a multimodal mixture-of-experts structure.

Visual and textual embeddings. Compared to modular MLLMs, Mono-InternVL directly patchifies images to input visual sequences using a lightweight module. Specifically, given the input image $I \in \mathbb{R}^{H \times W \times 3}$, the input visual embedding $x_v \in \mathbb{R}^{(h \times w) \times d}$ is obtained by

$$x_v = \text{MLP}(\text{PatchEmbed}(I) + \text{PE}). \quad (1)$$

Here, PatchEmbed($\cdot$) denotes a patch embedding layer with a stride of 28, meaning each visual token represents a 28×28 image patch. $\text{PE} \in \mathbb{R}^{(h \times w) \times d}$ is the learnable positional embedding as similar to InternVL-1.5 (Chen et al., 2024c). Besides, we also add an additional thumbnail to provide global visual information. After that, an MLP layer, *i.e.,* MLP($\cdot$), is used to project visual patches into the d-dimensional embedding space of the LLM. This simple visual tokenizer allows Mono-InternVL to process arbitrary-resolution images with up to 8 millions of pixels, *i.e.,* $10,240$ image patches, which can cover most high-resolution scenarios.

In Mono-InternVL, the textual tokenizer remains the same as the original one in the LLM. In particular, given the input text $T \in \mathbb{Z}^n$, we obtain textual embedding $x_t \in \mathbb{R}^{n \times d}$ by

$$x_t = \text{Tokenizer}(T). \quad (2)$$

Afterwards, the multimodal embedding is constructed as the concatenation of visual and textual embeddings, denoted as $x_m \in \mathbb{R}^{n' \times d}$.

Multimodal mixture-of-experts structure. The key principle of Mono-InternVL is to embed visual experts into a pre-trained LLM. In this case, Mono-InternVL can not only facilitate the visual pre-training with the pre-trained LLM knowledge, but also significantly mitigates the catastrophic forgetting issue during pre-training. Specifically, given the multimodal input $x_m \in \mathbb{R}^{n' \times d}$,
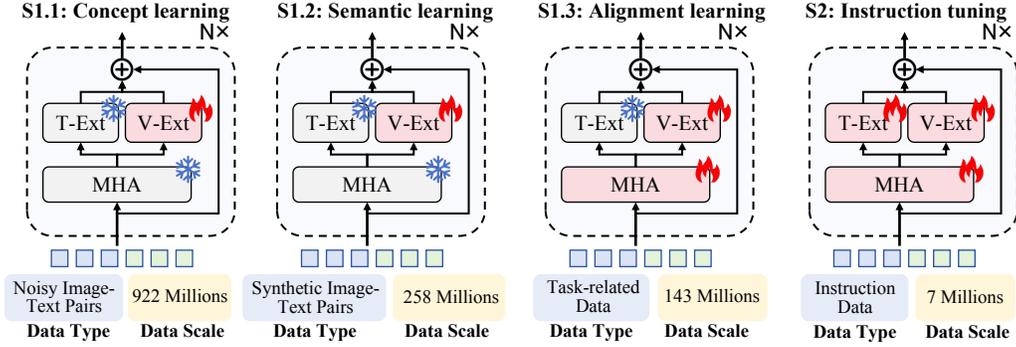
Figure 3: **The training recipe of Mono-InternVL.** In the first stage, Mono-Internvl is progressively pre-trained on massive data via three sub-stages (S1.1, S1.2, S1.3), where most parameters of LLM are frozen to preserve the pre-trained knowledge. In the second stage (S2), the entire model is optimized to accommodate various instructions.

a decoder-only LLM with a set of visual experts is used to generate the textual tokens step by step, which can be formulated by

$$p_s = \mathcal{F}_{\text{llm}}(y_s | x_m, y_{0:s-1}; \theta, \theta_v). \tag{3}$$

Here, $y \in \mathbb{R}^S$ and S denote the word length and its length, respectively. $p_s \in \mathbb{R}^m$ is the next-token probability and m is the size of word vocabulary. $\mathcal{F}_{\text{llm}}$ and θ denote the LLM and its pre-trained parameters, respectively. θ_v is the parameters of patch embedding layer and visual experts.

As shown in Fig. 2, $\mathcal{F}_{\text{llm}}$ is designed as a multimodal mixture-of-experts structure. In particular, we adopt the static routing strategy that assigns visual and textual experts to the corresponding tokens. Therefore, the l-th LLM layer can be defined by

$$\begin{aligned} x_m^{l'} &= x_m^{l-1} + \text{MHA}(\text{RMSNorm}(x_m^{l-1})), \\ x_m^{l} &= x_m^{l'} + \text{MMoE}(\text{RMSNorm}(x_m^{l'})). \end{aligned} \tag{4}$$

Here, MHA($\cdot$) and RMSNorm($\cdot$) denote the multi-head attention (Vaswani et al., 2017) and the layer normalization (Zhang & Sennrich, 2019), respectively. MMoE($\cdot$) is the proposed multimodal mixture-of-experts, formulated by

$$\text{MMoE}(x) = \begin{cases} \text{FFN}_v(x) & \text{if } x \in x_v, \\ \text{FFN}_t(x) & \text{if } x \in x_t. \end{cases} \tag{5}$$

Here, $x \in \mathbb{R}^d$ is the element of x_m. FFN$_v$ and FFN$_t$ denote the visual and textual experts, respectively. In practice, FFN$_v$ is initialized from the FFN$_t$ to leverage the pre-trained knowledge.

As defined in Eq. 4 and 5, the MMoE structure has two distinct advantages over the existing monolithic MLLM. Firstly, the visual learning of Mono-InternVL can greatly benefit from the pre-trained language knowledge, while the language ability can still be preserved by freezing FFN$_t$. Secondly, the MMoE structure significantly enhances the model's capacity for vision-and-language modeling, while the additional inference cost is almost negligible due to the MoE mechanism.

3.2 ENDOGENOUS VISUAL PRE-TRAINING

Endogenous Visual Pre-training (EViP) aims to maximize the benefits of Mono-InternVL from visual experts through pre-training on massive noisy and synthetic data. Unlike existing methods (Diao et al., 2024; ChameleonTeam, 2024), we formulate EViP from the perspective of delta tuning (Ding et al., 2022), in which most of the LLM parameters are frozen to preserve its pre-trained knowledge. Therefore, the objective of EViP can be defined by

$$\arg\min_{\Delta\theta} \mathcal{L}(\mathcal{F}_{\text{llm}}(x_m; \theta, \theta_v), \hat{y}), \tag{6}$$

where $\mathcal{L}(\cdot)$ and $\hat{y}$ denote the auto-regressive loss and the ground-truth, respectively. As shown in Fig. 3, $\Delta\theta$ denotes parameters of patch embedding and visual experts in the concept and semantic

Table 1: **Summary of datasets used in the endogenous visual pre-training.** In S1.2, caption for each image is synthetically produced by the pre-trained InternVL-8B (Chen et al., 2024c).

Stage	#Samples	Datasets
S1.1	922M	Laion-EN (en) (Schuhmann et al., 2022a), COYO (en) (Byeon et al., 2022)
S1.2	258M	Laion-EN (en) (Schuhmann et al., 2022a), COYO (en) (Byeon et al., 2022), SAM (en) (Kirillov et al., 2023)
S1.3	143M	**Captioning:** Laion-EN (en) (Schuhmann et al., 2022a), Laion-ZH (zh) (Schuhmann et al., 2022a), COYO (zh) (Byeon et al., 2022), GRIT (zh) (Peng et al., 2023), COCO (en) (Chen et al., 2015), TextCaps (en) (Sidorov et al., 2020) **Detection:** Objects365 (en&zh) (Shao et al., 2019), GRIT (en&zh) (Peng et al., 2023), All-Seeing (en&zh) (Wang et al., 2024a) **OCR (large):** Wukong-OCR (zh) (Gu et al., 2022), LaionCOCO-OCR (en) (Schuhmann et al., 2022b), Common Crawl PDF (en&zh) **OCR (small):** MMC-Inst (en) (Liu et al., 2023c), LSVT (zh) (Sun et al., 2019), ST-VQA (en) (Biten et al., 2019), RCTW-17 (zh) (Shi et al., 2017), ReCTs (zh) (Zhang et al., 2019), ArT (en&zh) (Chng et al., 2019), SynthDoG (en&zh) (Kim et al., 2022), COCO-Text (en) (Veit et al., 2016), ChartQA (en) (Masry et al., 2022), CTW (zh) (Yuan et al., 2019), DocVQA (en) (Clark & Gardner, 2018), TextOCR (en) (Singh et al., 2021), PlotQA (en) (Methani et al., 2020), InfoVQA (en) (Mathew et al., 2022)

learning, *i.e.,* θ_v, while in the alignment learning stage $\Delta\theta$ also includes the parameters of multi-head attentions. Based on Eq. 6, EViP is designed as a progressive learning process. As shown in Fig. 3 and Tab. 1, EViP consists of three sub-stages, namely concept learning (S1.1), semantic learning (S1.2) and alignment learning (S1.3). For different sub-stages, we use carefully partitioned data to achieve coarse-to-fine visual learning.

Concept learning. Concept learning aims to encourage the model to learn fundamental visual concepts, such as object categories or basic shapes. Therefore, we first pre-train Mono-InternVL with about 922 million noisy samples, which are sampled from Laion-2B (Schuhmann et al., 2022a) and Coyo-700M (Byeon et al., 2022). In this sub-stage, Mono-InternVL employs a simple prompt to perform generative learning, *i.e.,* "provide a one-sentence caption for the image". Meanwhile, we constrain the maximum number of image patches of the visual tokenizer to 1,280 for training efficiency. To ensure that the foundational language capabilities are preserved while enabling visual specialization, the entire LLM is kept frozen during concept learning, and only the patch embedding and visual experts are optimized.

Semantic learning. After concept learning, Mono-InternVL is able to understand basic concepts in the image, but organizing this information to produce reasonable descriptions remains challenging. To achieve a higher-level visual understanding, we utilize the pre-trained InternVL-8B (Chen et al., 2024c) to produce short captions for 258 million images. Compared to the original noisy captions, synthetic captions typically depict complex visual knowledge, such as relationship and world knowledge, *etc.*, while containing less noisy information unrelated to the image, *e.g.,* time of shooting, and the photographer. In this sub-stage, we adopt the same optimization strategy as concept learning, except that the maximum number of image patches is increased to 1,792.

Alignment learning. To meet the visual requirements of downstream tasks, we further perform alignment learning on Mono-InternVL. As shown in Tab. 1, our alignment data is sampled from the pre-training data of InternVL-1.5 (Chen et al., 2024c), including 143 million samples of image captioning, detection and optical character recognition (OCR). In particular, captioning data, detection data and OCR data account for about 53.9%, 5.2% and 40.9% of the total, respectively. In this sub-stage, we utilize the task-specific prompts from InternVL-1.5 for the generative learning, and increase the maximum number of image patches to 3,328. Compared to previous sub-stages, the multi-head attention layers are additionally optimized to achieve better vision-language alignment.

3.3 INSTRUCTION TUNING

In this stage, we follow InternVL (Chen et al., 2024c) to use around 5 million bilingual instructions for supervised learning, covering various tasks such as visual question answering, multimodal dialogue, mathematics, knowledge, *etc*. In addition to this, we further include additional instruction data for video understanding and handwritten text recognition. In this stage, the entire models

Table 2: **Comparison with existing MLLMs on general MLLM benchmarks.** "#A-Param" denotes the number of activated parameters. For MME, we sum the perception and cognition scores. Average scores are computed by normalizing each metric to a range between 0 and 100.

Model	#A-Param	MMB	MMVet	MMMU	MME	MathVista	SEED-I	OCRBench	HallB	CCB	Avg
Modular MLLMs:											
MobileVLM-V2-1.7B	1.7B	57.7	—	—	—	—	—	—	—	—	—
MobileVLM-V2-3B	3.0B	63.2	—	—	—	—	—	—	—	—	—
Mini-Gemini-2B	3.5B	59.8	31.1	31.7	1653	29.4	—	—	—	—	—
MM1-3B-MoE-Chat	3.5B	70.8	42.2	38.6	1772	32.6	69.4	—	—	—	—
DeepSeek-VL-1.3B	2.0B	64.6	34.8	32.2	1532	31.1	66.7	409	27.6	37.6	43.4
PaliGemma-3B	2.9B	71.0	33.1	34.9	1686	28.7	69.6	614	32.2	29.6	46.7
MiniCPM-V	2.8B	64.1	31.1	38.3	1650	28.9	65.6	366	36.2	41.4	44.6
MiniCPM-V-2	2.8B	69.1	41.0	38.2	1809	38.7	67.1	605	36.1	45.3	51.2
InternVL-1.5-2B	2.2B	70.9	39.3	34.6	1902	41.1	69.8	654	37.5	63.5	54.4
Monolithic MLLMs:											
Fuyu-8B (HD)	8B	10.7	21.4	—	—	—	—	—	—	—	—
SOLO	7B	—	—	—	1260	34.4	64.4	—	—	—	—
Chameleon-7B[1]	7B	31.1	8.3	25.4	170	22.3	30.6	7	17.1	3.5	16.1
EVE-7B	7B	49.5	25.6	32.3	1483	25.2	61.3	327	21.1	12.4	34.8
EVE-7B (HD)	7B	52.3	25.7	32.6	1628	34.2	64.6	398	26.4	16.3	38.9
Emu3	8B	58.5	37.2	31.6	—	—	**68.2**	687	—	—	—
Mono-InternVL-2B	1.8B	**65.5**	**40.1**	33.7	1875	**45.7**	67.4	**767**	34.8	66.3	**55.2**

are optimized and the maximum number of image patches is increased to 6,400 to accommodate high-resolution images. Details of instruction data can be found in Appendix §A.1.

4 EXPERIMENTS

4.1 EVALUATION BENCHMARKS

We evaluate Mono-InternVL and existing MLLMs on 16 comprehensive multimodal benchmarks. Specifically, general MLLM benchmarks encompass MMBench-EN *test* (Liu et al., 2023f), MMVet (Yu et al., 2023b), MMMU *val* (Yue et al., 2023), MME (Fu et al., 2023), MathVista *test-mini* (Lu et al., 2023), SEED Image (Ge et al., 2024), OCRBench (Liu et al., 2023g), Hallusion-Bench (Guan et al., 2023), and CCBench *dev* (Liu et al., 2023f). Visual question answering benchmarks include TextVQA *val* (Singh et al., 2019), SQA *test* (Lu et al., 2022a), GQA *test-dev* (Hudson & Manning, 2019), DocVQA *test* (Clark & Gardner, 2018), AI2D *test* (Kembhavi et al., 2016), ChartQA *test* (Masry et al., 2022), and InfographicVQA *test* (Mathew et al., 2022). The evaluation metrics follow the existing methods (Chen et al., 2024c; Diao et al., 2024). Part of the results of Chameleon and EVE are evaluated with VLMEvalKit (Duan et al., 2024) or from the OpenCompass leaderboard (Contributors, 2023).

4.2 IMPLEMENTATION DETAILS

Mono-InternVL is implemented based on InternLM2-1.8B (Cai et al., 2024) with newly added visual tokenizer and visual experts. The visual experts are initialized from pre-trained MLPs in InternLM2-1.8B to leverage existing learned representations for improved visual feature extraction, which accounts for 1.2 billion parameters. We adopt a similar dynamic high-resolution strategy from InternVL-1.5 (Chen et al., 2024c) to align an optimal resolution for input image, which is then patchfied to visual tokens. The remaining configurations are kept identical to InternLM2-1.8B. The endogenous visual pre-training and instruction tuning take approximately 16 days (646*k* iterations) and 1 day (14*k* iterations) on 256 NVIDIA A100 GPUs, respectively. More detailed training configurations are given in Appendix §A.2.

---

[1]Chameleon-7B frequently rejects to perform the task with a response of "I can't help you with this", thus resulting in poor performance.

Table 3: **Comparison with existing MLLMs on visual question answering benchmarks.**

Model	#A-Param	TextVQA	SQA-I	GQA	DocVQA	AI2D	ChartQA	InfoVQA	Avg
Modular MLLMs:									
MobileVLM-V2-1.7B	1.7B	52.1	66.7	59.3	–	–	–	–	–
MobileVLM-V2-3B	3.0B	57.5	70.0	66.1	–	–	–	–	–
Mini-Gemini-2B	3.5B	56.2	–	–	34.2	–	–	–	–
MM1-3B-MoE-Chat	3.5B	72.9	76.1	–	–	–	–	–	–
DeepSeek-VL-1.3B	2.0B	57.8	–	–	–	51.5	–	–	–
PaliGemma-3B	2.9B	68.1	–	–	–	68.3	–	–	–
MiniCPM-V	2.8B	60.6	–	–	38.2	56.3	–	–	–
MiniCPM-V-2	2.8B	74.1	–	–	71.9	62.9	–	–	–
InternVL-1.5-2B	2.2B	70.5	84.9	61.6	85.0	69.8	74.8	55.4	71.7
Monolithic MLLMs:									
Fuyu-8B (HD)	8B	–	–	–	–	64.5	–	–	–
SOLO	7B	–	73.3	–	–	61.4	–	–	–
Chameleon-7B[1]	7B	4.8	47.2	–	1.5	46.0	2.9	5.0	17.9
EVE-7B	7B	51.9	63.0	60.8	22.0	48.5	19.5	20.0	40.8
EVE-7B (HD)	7B	56.8	64.9	**62.6**	53.0	61.0	59.1	25.0	54.6
Emu3	8B	64.7	89.2	60.3	76.3	**70.0**	68.6	**43.8**	67.6
Mono-InternVL-2B	1.8B	**72.6**	**93.6**	59.5	**80.0**	68.6	**73.7**	43.0	**70.1**

Table 4: **Zero-shot pre-training performance of Mono-InternVL and existing MLLMs.** "S1.2" and "S1.3" denote pre-training stages of semantic learning and alignment learning, respectively. Images of COCO have been seen in Mono-InternVL-S1.3, so we mark its performance in gray.

Model	#A-Param	Data	Shots	COCO Caps	Flickr30k	NoCaps	VQAv2
Flamingo	3B	>2.1B	0	73.0	–	–	49.2
MM1	3.5B	>2.3B	0	73.5	–	55.6	46.2
Chameleon	34B	>1.4B	2	120.2	74.7	–	66.0
Mono-InternVL-S1.2	1.8B	0.9B	0	87.3	72.7	54.1	–
Mono-InternVL-S1.3	1.8B	1.1B	0	135.6	77.3	116.5	71.1

4.3 QUANTITATIVE EXPERIMENTS

Comparison with existing MLLMs. In Tab. 2 and 3, we compare Mono-InternVL and existing MLLMs on 16 multimodal benchmarks. From Tab. 2, the first observation is that most modular MLLMs outperform existing monolithic MLLMs by significant margins. For example, the average performance of InternVL-1.5-2B (Chen et al., 2024c) on 9 MLLM benchmarks greatly exceeds the SoTA monolithic MLLM, *i.e.,* + 15.5% over EVE-7B (HD) (Diao et al., 2024). These results strongly suggest the challenges in existing monolithic MLLMs. In contrast, Mono-InternVL-2B with a slightly smaller model size can even outperform the SoTA modular MLLM, *i.e.,* + 0.8% against InternVL-1.5-2B on average. Notably, Mono-InternVL-2B demonstrates distinct advantages on MathVista and OCRBench, suggesting its seamless text recognition and reasoning capabilities. Moreover, superior bilingual ability of Mono-InternVL-2B is also validated on CCBench, which contains a large amount of questions related to Chinese culture. Compared to existing monolithic MLLMs, performance gains of Mono-InternVL are more distinct, *e.g.,* +15.4% over EVE-7B (HD) (Diao et al., 2024) on MMVet and +7.9% over Emu3 (Wang et al., 2024b) on TextVQA, while using a much smaller parameter scale. Similar advantages of Mono-InternVL can also been witnessed in Tab. 3, *e.g.,* +2.1% on TextVQA. Nevertheless, we also observe that Mono-InternVL is still inferior to InternVL-1.5 on high-resolution benchmarks, *e.g.,* -12.4% on InfoVQA. This is because specific optimizations for high-resolution encoding are not the focus of the paper, *e.g.,* positional embedding and high-resolution training data, which we plan to explore in future research. Overall, these comparisons significantly validate the architecture and training strategy of Mono-InternVL.

In Tab. 4, we further compare the pre-training performance of Mono-InternVL and existing MLLMs. From this table, we can observe that with concept and semantic learning, Mono-InternVL-S1.2

Table 5: **Ablation of different strategies for visual pre-training.** All models are pre-trained on 61 million image-text pairs from Laion-2B (Schuhmann et al., 2022a) and fine-tuned on instruction data from LLaVA-665k. (Liu et al., 2023d). "Full" and "Delta" denote full tuning and delta tuning, respectively. "T-Param" refers to trainable parameters.

Model	#T-Param	Strategy	MME-P	DocVQA	InfoVQA	SQA-I	GQA	ChartQA	AI2D
InternLM2	1.8B	Full	753	16.1	11.6	36.7	51.4	10.8	27.7
+ V-Expert	3.0B	Full	948	18.6	11.9	37.7	53.0	11.1	26.6
+ V-Expert	1.2B	Delta	995	18.9	14.6	56.5	53.4	13.5	42.7
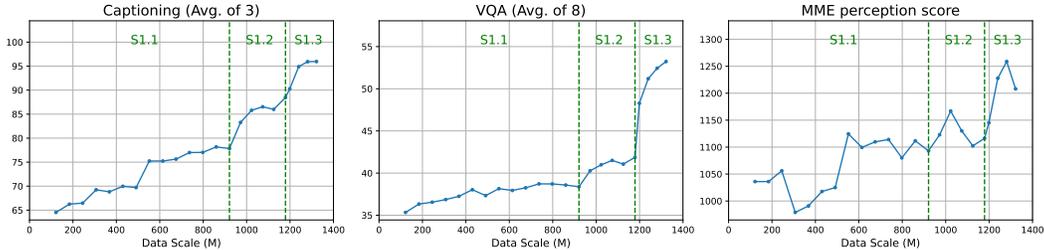
Figure 4: **Downstream performance breakdown with the increase of pre-training data size across three sub-stages: (S1.1) Concept learning; (S1.2) Semantic learning; (S1.3) Alignment learning.** For each data point, we fine-tune the corresponding pre-trained model on the instruction data of LLaVA-665k and obtain the downstream performance. Results of captioning and VQA are averaged from 3 and 8 tasks, respectively. See Appendix §A.3 for complete results.

already exceeds existing modular MLLMs, *e.g.,* +13.8 CIDEr over MM1 (McKinzie et al., 2024) on COCO Captions, demonstrating that Mono-InternVL-S1.2 is effective in capturing fundamental multimodal relationships. It is worth noting that pre-training in Mono-InternVL-S1.2 only consumes about 0.9B image-text pairs, but the cost in MM1 and Flamingo is much more expensive, *e.g.,* more than 2B data. Compared to monolithic MLLMs, Mono-InternVL also demonstrates superior performance. For instance, even though Chameleon has a much larger model size, it is still inferior to Mono-InternVL-S1.3 by -2.6 CIDEr on Flickr30k (Young et al., 2014). These results further confirm the effectiveness of EViP for Mono-InternVL.

Ablation studies. To validate the design of Mono-InternVL, we conduct extensive ablation studies in Tab. 5 and Fig. 4. Specifically, Tab. 5 compares different strategies for visual pre-training. The first row is the common strategy used in existing monolithic MLLMs, *i.e.,* full tuning of the LLM, which yields the worst downstream performance in the table. After employing visual experts (the second row), such a full-tuning strategy becomes more effective, *e.g.,* +1.6% on GQA. These comparisons well validate that the shared architecture for joint vision and language modeling is sub-optimal in monolithic MLLMs. Besides, we also observe that the delta tuning strategy greatly benefits the visual pre-training, providing +18.8% and 16.1% gains on SQA-I and AI2D, respectively. Compared to full tuning, delta tuning can effectively preserve the knowledge of the pre-trained LLM, which is also crucial for maintaining the language understanding capabilities required for effective multimodal interactions.

Fig. 4 further demonstrates the relationship between downstream performance and pre-training data size. From it we can observe that performance of Mono-InternVL will gradually reach an upper bound in the concept learning. Through additional semantic learning and alignment learning, capabilities of Mono-InternVL consistently boost as the data size increases. It is important to note that that the alignment learning plays a significant role for VQA and MME, which can provide sufficient task-related knowledge, *e.g.,* OCR knowledge. These results not only demonstrate the data scalability of Mono-InternVL, but also confirm the advantages of coarse-to-fine learning in EViP.

Comparison of inference efficiency. In Tab. 6, we compare the inference speed of Mono-InternVL and InternVL-1.5 using the popular deployment library LMDeploy (LMDeployContributors, 2023). From this table, we can find that due to the elimination of visual encoder, Mono-InternVL demonstrates superior efficiency under different number of input tokens. In particular, the first-token time is greatly reduced in Mono-InternVL, *e.g.,* up to -67% against InternVL-1.5. Benefiting from this, the overall throughput is correspondingly increased by around 31%. These results greatly validate

Table 6: **Inference speed comparison of Mono-InternVL and InternVL-1.5.** Models are deployed on an NVIDIA A100 using LMDeploy with Pytorch backend (LMDeployContributors, 2023), with a concurrency of 16 and the number of output tokens fixed as 120. "TTFT" and "TPS" denotes the time to first token in seconds and throughput in tokens per second, respectively.

Model	#Image Tokens	#Text Tokens	#Total Input Tokens	TTFT	TPS
InternVL-1.5-2B	768	256	1024	0.24	382
Mono-InternVL-2B	768	256	1024	0.09 (-63%)	436 (+14%)
InternVL-1.5-2B	1792	256	2048	0.45	183
Mono-InternVL-2B	1792	256	2048	0.15 (-67%)	232 (+27%)
InternVL-1.5-2B	3840	256	4096	1.93	52
Mono-InternVL-2B	3840	256	4096	0.79 (-59%)	68 (+31%)
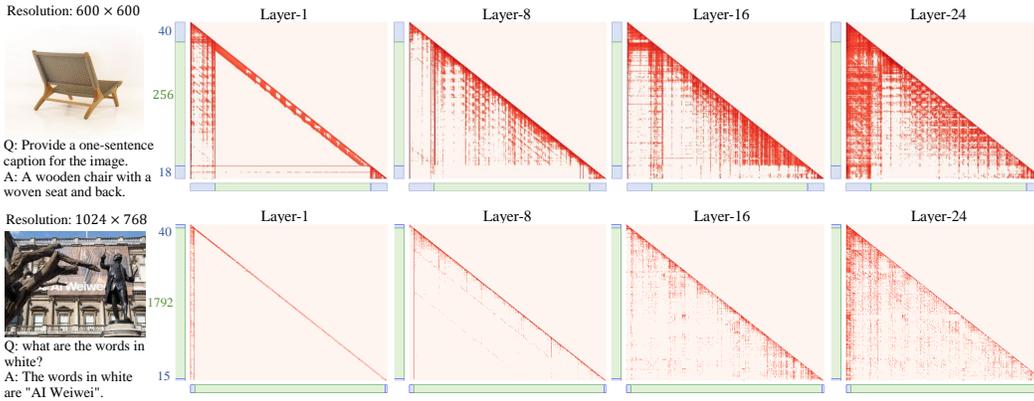
Figure 5: **Visualization of attention maps in Mono-InternVL.** The first blue segment, green segment and the second green segment in the axes represent the system prompt tokens (text), image tokens (visual) and user prompt tokens (text), respectively. The numbers on the left side of attention maps indicate the number of tokens.

the efficiency of Mono-InternVL. We note that this is only an initial attempt, and using Turbomind backend or further optimization techniques may yield better performance.

4.4 QUALITATIVE EXPERIMENTS

To gain in-depth insights into Mono-InternVL, we visualize its attention maps of different layers in Fig. 5. From this figure, we can draw two noteworthy findings. Firstly, despite the global connectivity of the Transformer architecture, locality still exists in the visual encoding of shallow layers. As shown in Fig. 5, in the first layer, visual tokens only interact with their nearby content, yielding patterns that closely resemble those produced by convolutional neural networks (He et al., 2016). Secondly, modalities are barely interactive at shallow layers but gradually fused as the layers deepen. As illustrated in Fig. 5, the attention weights between visual and textual tokens are extremely small in the first layer and become larger in deeper layers. We believe these examples will provide useful hints for the design of monolithic MLLMs. More examples are given in Appendix §A.4.

5 CONCLUSION

In this paper, we propose Mono-InternVL, a monolithic multimodal large language model (MLLM) that integrates visual encoding and textual decoding into a single LLM. In Mono-InternVL, a set of visual experts is embedded into the pre-trained LLM via a mixture-of-experts mechanism. By freezing the LLM, Mono-InternVL ensures that visual capabilities are optimized without compromising the pre-trained language knowledge. Based on this structure, an innovative Endogenous Visual Pre-training (EViP) is introduced to realize coarse-to-fine visual learning. Extensive experiments demonstrate the effectiveness and efficiency of Mono-InternVL compared to existing MLLMs. Our work greatly pushes the boundaries of monolithic MLLMs, providing new possibilities for the development of MLLMs.

REFERENCES

Jinze Bai, Shuai Bai, Yunfei Chu, Zeyu Cui, Kai Dang, Xiaodong Deng, Yang Fan, Wenbin Ge, Yu Han, Fei Huang, Binyuan Hui, Luo Ji, Mei Li, Junyang Lin, Runji Lin, Dayiheng Liu, Gao Liu, Chengqiang Lu, Keming Lu, Jianxin Ma, Rui Men, Xingzhang Ren, Xuancheng Ren, Chuanqi Tan, Sinan Tan, Jianhong Tu, Peng Wang, Shijie Wang, Wei Wang, Shengguang Wu, Benfeng Xu, Jin Xu, An Yang, Hao Yang, Jian Yang, Shusheng Yang, Yang Yao, Bowen Yu, Hongyi Yuan, Zheng Yuan, Jianwei Zhang, Xingxuan Zhang, Yichang Zhang, Zhenru Zhang, Chang Zhou, Jingren Zhou, Xiaohuan Zhou, and Tianhang Zhu. Qwen technical report. *arXiv: 2309.16609*, 2023a.

Jinze Bai, Shuai Bai, Shusheng Yang, Shijie Wang, Sinan Tan, Peng Wang, Junyang Lin, Chang Zhou, and Jingren Zhou. Qwen-vl: A frontier large vision-language model with versatile abilities. *arXiv preprint arXiv:2308.12966*, 2023b.

Yuelin Bai, Xinrun Du, Yiming Liang, Yonggang Jin, Ziqiang Liu, Junting Zhou, Tianyu Zheng, Xincheng Zhang, Nuo Ma, Zekun Wang, et al. Coig-cqia: Quality is all you need for chinese instruction fine-tuning. *arXiv preprint arXiv:2403.18058*, 2024.

Hangbo Bao, Wenhui Wang, Li Dong, Qiang Liu, Owais Khan Mohammed, Kriti Aggarwal, Subhojit Som, Songhao Piao, and Furu Wei. Vlmo: Unified vision-language pre-training with mixture-of-modality-experts. *Advances in Neural Information Processing Systems*, 35:32897–32912, 2022.

Rohan Bavishi, Erich Elsen, Curtis Hawthorne, Maxwell Nye, Augustus Odena, Arushi Somani, and Sağnak Taşırlar. Introducing our multimodal models, 2023. URL https://www.adept.ai/blog/fuyu-8b.

Lucas Beyer, Andreas Steiner, André Susano Pinto, Alexander Kolesnikov, Xiao Wang, Daniel Salz, Maxim Neumann, Ibrahim Alabdulmohsin, Michael Tschannen, Emanuele Bugliarello, et al. Paligemma: A versatile 3b vlm for transfer. *arXiv preprint arXiv:2407.07726*, 2024.

Ali Furkan Biten, Ruben Tito, Andres Mafla, Lluis Gomez, Marçal Rusinol, Ernest Valveny, CV Jawahar, and Dimosthenis Karatzas. Scene text visual question answering. In *ICCV*, pp. 4291–4301, 2019.

Minwoo Byeon, Beomhee Park, Haecheon Kim, Sungjun Lee, Woonhyuk Baek, and Saehoon Kim. Coyo-700m: Image-text pair dataset. https://github.com/kakaobrain/coyo-dataset, 2022.

Zheng Cai, Maosong Cao, Haojiong Chen, Kai Chen, Keyu Chen, Xin Chen, Xun Chen, Zehui Chen, Zhi Chen, Pei Chu, et al. Internlm2 technical report. *arXiv preprint arXiv:2403.17297*, 2024.

Jie Cao and Jing Xiao. An augmented benchmark dataset for geometric question answering through dual parallel text encoding. In *COLING*, pp. 1511–1520, 2022.

ChameleonTeam. Chameleon: Mixed-modal early-fusion foundation models. *arXiv preprint arXiv:2405.09818*, 2024.

Guiming Hardy Chen, Shunian Chen, Ruifei Zhang, Junying Chen, Xiangbo Wu, Zhiyi Zhang, Zhihong Chen, Jianquan Li, Xiang Wan, and Benyou Wang. Allava: Harnessing gpt4v-synthesized data for a lite vision-language model. *arXiv preprint arXiv:2402.11684*, 2024a.

Xinlei Chen, Hao Fang, Tsung-Yi Lin, Ramakrishna Vedantam, Saurabh Gupta, Piotr Dollár, and C Lawrence Zitnick. Microsoft coco captions: Data collection and evaluation server. *arXiv preprint arXiv:1504.00325*, 2015.

Yangyi Chen, Xingyao Wang, Hao Peng, and Heng Ji. A single transformer for scalable vision-language modeling. *arXiv preprint arXiv:2407.06438*, 2024b.

Zhe Chen, Jiannan Wu, Wenhai Wang, Weijie Su, Guo Chen, Sen Xing, Muyan Zhong, Qinglong Zhang, Xizhou Zhu, Lewei Lu, Bin Li, Ping Luo, Tong Lu, Yu Qiao, and Jifeng Dai. Internvl: Scaling up vision foundation models and aligning for generic visual-linguistic tasks. *arXiv: 2312.14238*, 2023.

Zhe Chen, Weiyun Wang, Hao Tian, Shenglong Ye, Zhangwei Gao, Erfei Cui, Wenwen Tong, Kongzhi Hu, Jiapeng Luo, Zheng Ma, et al. How far are we to gpt-4v? closing the gap to commercial multimodal models with open-source suites. *arXiv:2404.16821*, 2024c.

Chee Kheng Chng, Yuliang Liu, Yipeng Sun, Chun Chet Ng, Canjie Luo, Zihan Ni, ChuanMing Fang, Shuaitao Zhang, Junyu Han, Errui Ding, et al. Icdar2019 robust reading challenge on arbitrary-shaped text-rrc-art. In *ICDAR*, pp. 1571–1576, 2019.

Xiangxiang Chu, Limeng Qiao, Xinyu Zhang, Shuang Xu, Fei Wei, Yang Yang, Xiaofei Sun, Yiming Hu, Xinyang Lin, Bo Zhang, et al. Mobilevlm v2: Faster and stronger baseline for vision language model. *arXiv preprint arXiv:2402.03766*, 2024.

Christopher Clark and Matt Gardner. Simple and effective multi-paragraph reading comprehension. In *ACL*, pp. 845–855, 2018.

Contributors. Opencompass: A universal evaluation platform for foundation models. https://github.com/open-compass/opencompass, 2023.

Wenliang Dai, Junnan Li, Dongxu Li, Anthony Meng Huat Tiong, Junqi Zhao, Weisheng Wang, Boyang Li, Pascale Fung, and Steven C. H. Hoi. Instructblip: Towards general-purpose vision-language models with instruction tuning. In *NeurIPS*, 2023.

Abhishek Das, Satwik Kottur, Khushi Gupta, Avi Singh, Deshraj Yadav, José MF Moura, Devi Parikh, and Dhruv Batra. Visual dialog. In *CVPR*, pp. 326–335, 2017.

Mostafa Dehghani, Josip Djolonga, Basil Mustafa, Piotr Padlewski, Jonathan Heek, Justin Gilmer, Andreas Peter Steiner, Mathilde Caron, Robert Geirhos, Ibrahim Alabdulmohsin, Rodolphe Jenatton, Lucas Beyer, Michael Tschannen, Anurag Arnab, Xiao Wang, Carlos Riquelme Ruiz, Matthias Minderer, Joan Puigcerver, Utku Evci, Manoj Kumar, Sjoerd van Steenkiste, Gamaleldin Fathy Elsayed, Aravindh Mahendran, Fisher Yu, Avital Oliver, Fantine Huot, Jasmijn Bastings, Mark Collier, Alexey A. Gritsenko, Vighnesh Birodkar, Cristina Nader Vasconcelos, Yi Tay, Thomas Mensink, Alexander Kolesnikov, Filip Pavetic, Dustin Tran, Thomas Kipf, Mario Lucic, Xiaohua Zhai, Daniel Keysers, Jeremiah J. Harmsen, and Neil Houlsby. Scaling vision transformers to 22 billion parameters. In *ICML*, volume 202, pp. 7480–7512, 2023.

Haiwen Diao, Yufeng Cui, Xiaotong Li, Yueze Wang, Huchuan Lu, and Xinlong Wang. Unveiling encoder-free vision-language models. *arXiv preprint arXiv:2406.11832*, 2024.

Ning Ding, Yujia Qin, Guang Yang, Fuchao Wei, Zonghan Yang, Yusheng Su, Shengding Hu, Yulin Chen, Chi-Min Chan, Weize Chen, et al. Delta tuning: A comprehensive study of parameter efficient methods for pre-trained language models. *arXiv preprint arXiv:2203.06904*, 2022.

Alexey Dosovitskiy, Lucas Beyer, Alexander Kolesnikov, Dirk Weissenborn, Xiaohua Zhai, Thomas Unterthiner, Mostafa Dehghani, Matthias Minderer, Georg Heigold, Sylvain Gelly, Jakob Uszkoreit, and Neil Houlsby. An image is worth 16x16 words: Transformers for image recognition at scale. In *ICLR*, 2021.

Haodong Duan, Junming Yang, Yuxuan Qiao, Xinyu Fang, Lin Chen, Yuan Liu, Xiaoyi Dong, Yuhang Zang, Pan Zhang, Jiaqi Wang, Dahua Lin, and Kai Chen. Vlmevalkit: An open-source toolkit for evaluating large multi-modality models, 2024. URL https://arxiv.org/abs/2407.11691.

Chaoyou Fu, Peixian Chen, Yunhang Shen, Yulei Qin, Mengdan Zhang, Xu Lin, Zhenyu Qiu, Wei Lin, Jinrui Yang, Xiawu Zheng, Ke Li, Xing Sun, and Rongrong Ji. MME: A comprehensive evaluation benchmark for multimodal large language models. *arXiv: 2306.13394*, 2023.

Yuying Ge, Sijie Zhao, Ziyun Zeng, Yixiao Ge, Chen Li, Xintao Wang, and Ying Shan. Making LLaMA SEE and draw with SEED tokenizer. In *The Twelfth International Conference on Learning Representations*, 2024. URL https://openreview.net/forum?id=0Nui91LBQS.

Yash Goyal, Tejas Khot, Douglas Summers-Stay, Dhruv Batra, and Devi Parikh. Making the V in VQA matter: Elevating the role of image understanding in visual question answering. In *CVPR*, pp. 6325–6334, 2017.

Jiaxi Gu, Xiaojun Meng, Guansong Lu, Lu Hou, Niu Minzhe, Xiaodan Liang, Lewei Yao, Runhui Huang, Wei Zhang, Xin Jiang, et al. Wukong: A 100 million large-scale chinese cross-modal pre-training benchmark. *NeurIPS*, 35:26418–26431, 2022.

Tianrui Guan, Fuxiao Liu, Xiyang Wu, Ruiqi Xian, Zongxia Li, Xiaoyu Liu, Xijun Wang, Lichang Chen, Furong Huang, Yaser Yacoob, et al. Hallusionbench: An advanced diagnostic suite for entangled language hallucination & visual illusion in large vision-language models. *arXiv: 2310.14566*, 2023.

Jean-Philippe Thiran Guillaume Jaume, Hazim Kemal Ekenel. Funsd: A dataset for form understanding in noisy scanned documents. In *Accepted to ICDAR-OST*, 2019.

Conghui He, Zhenjiang Jin, Chao Xu, Jiantao Qiu, Bin Wang, Wei Li, Hang Yan, Jiaqi Wang, and Dahua Lin. Wanjuan: A comprehensive multimodal dataset for advancing english and chinese large models. *arXiv preprint arXiv:2308.10755*, 2023.

Kaiming He, Xiangyu Zhang, Shaoqing Ren, and Jian Sun. Deep residual learning for image recognition. In *CVPR*, pp. 770–778, 2016.

Zheng Huang, Kai Chen, Jianhua He, Xiang Bai, Dimosthenis Karatzas, Shijian Lu, and CV Jawahar. Icdar2019 competition on scanned receipt ocr and information extraction. In *2019 International Conference on Document Analysis and Recognition (ICDAR)*, pp. 1516–1520. IEEE, 2019.

Drew A. Hudson and Christopher D. Manning. GQA: A new dataset for real-world visual reasoning and compositional question answering. In *CVPR*, pp. 6700–6709, 2019.

Baoxiong Jia, Ting Lei, Song-Chun Zhu, and Siyuan Huang. Egotaskqa: Understanding human tasks in egocentric videos. *Advances in Neural Information Processing Systems*, 35:3343–3360, 2022.

Kushal Kafle, Brian Price, Scott Cohen, and Christopher Kanan. Dvqa: Understanding data visualizations via question answering. In *CVPR*, pp. 5648–5656, 2018.

Aniruddha Kembhavi, Mike Salvato, Eric Kolve, Minjoon Seo, Hannaneh Hajishirzi, and Ali Farhadi. A diagram is worth a dozen images. In *ECCV*, pp. 235–251, 2016.

Aniruddha Kembhavi, Minjoon Seo, Dustin Schwenk, Jonghyun Choi, Ali Farhadi, and Hannaneh Hajishirzi. Are you smarter than a sixth grader? textbook question answering for multimodal machine comprehension. In *CVPR*, pp. 4999–5007, 2017.

Geewook Kim, Teakgyu Hong, Moonbin Yim, JeongYeon Nam, Jinyoung Park, Jinyeong Yim, Wonseok Hwang, Sangdoo Yun, Dongyoon Han, and Seunghyun Park. Ocr-free document understanding transformer. In *ECCV*, 2022.

Alexander Kirillov, Eric Mintun, Nikhila Ravi, Hanzi Mao, Chloé Rolland, Laura Gustafson, Tete Xiao, Spencer Whitehead, Alexander C. Berg, Wan-Yen Lo, Piotr Dollár, and Ross B. Girshick. Segment anything. *arXiv: 2304.02643*, 2023.

Ranjay Krishna, Yuke Zhu, Oliver Groth, Justin Johnson, Kenji Hata, Joshua Kravitz, Stephanie Chen, Yannis Kalantidis, Li-Jia Li, David A. Shamma, Michael S. Bernstein, and Li Fei-Fei. Visual genome: Connecting language and vision using crowdsourced dense image annotations. *IJCV*, 123(1):32–73, 2017.

Jianfeng Kuang, Wei Hua, Dingkang Liang, Mingkun Yang, Deqiang Jiang, Bo Ren, and Xiang Bai. Visual information extraction in the wild: practical dataset and end-to-end solution. In *International Conference on Document Analysis and Recognition*, pp. 36–53. Springer, 2023.

LAION. Gpt-4v dataset. https://huggingface.co/datasets/laion/gpt4v-dataset, 2023.

Paul Lerner, Olivier Ferret, Camille Guinaudeau, Hervé Le Borgne, Romaric Besançon, José G Moreno, and Jesús Lovón Melgarejo. Viquae, a dataset for knowledge-based visual question answering about named entities. In *SIGIR*, pp. 3108–3120, 2022.

Junnan Li, Dongxu Li, Caiming Xiong, and Steven C. H. Hoi. BLIP: bootstrapping language-image pre-training for unified vision-language understanding and generation. In *ICLR*, volume 162, pp. 12888–12900, 2022.

Junnan Li, Dongxu Li, Silvio Savarese, and Steven C. H. Hoi. BLIP-2: bootstrapping language-image pre-training with frozen image encoders and large language models. In *ICML*, volume 202, pp. 19730–19742, 2023a.

KunChang Li, Yinan He, Yi Wang, Yizhuo Li, Wenhai Wang, Ping Luo, Yali Wang, Limin Wang, and Yu Qiao. Videochat: Chat-centric video understanding. *arXiv preprint arXiv:2305.06355*, 2023b.

Yanwei Li, Yuechen Zhang, Chengyao Wang, Zhisheng Zhong, Yixin Chen, Ruihang Chu, Shaoteng Liu, and Jiaya Jia. Mini-gemini: Mining the potential of multi-modality vision language models. *arXiv: 2403.18814*, 2024.

Zhuowan Li, Xingrui Wang, Elias Stengel-Eskin, Adam Kortylewski, Wufei Ma, Benjamin Van Durme, and Alan L Yuille. Super-clevr: A virtual benchmark to diagnose domain robustness in visual reasoning. In *CVPR*, pp. 14963–14973, 2023c.

Xi Victoria Lin, Akshat Shrivastava, Liang Luo, Srinivasan Iyer, Mike Lewis, Gargi Gosh, Luke Zettlemoyer, and Armen Aghajanyan. Moma: Efficient early-fusion pre-training with mixture of modality-aware experts. *arXiv preprint arXiv:2407.21770*, 2024.

Adam Dahlgren Lindström and Savitha Sam Abraham. Clevr-math: A dataset for compositional language, visual and mathematical reasoning. *arXiv preprint arXiv:2208.05358*, 2022.

Fangyu Liu, Guy Emerson, and Nigel Collier. Visual spatial reasoning. *TACL*, 11:635–651, 2023a.

Fuxiao Liu, Kevin Lin, Linjie Li, Jianfeng Wang, Yaser Yacoob, and Lijuan Wang. Aligning large multi-modal model with robust instruction tuning. *arXiv preprint arXiv:2306.14565*, 2023b.

Fuxiao Liu, Xiaoyang Wang, Wenlin Yao, Jianshu Chen, Kaiqiang Song, Sangwoo Cho, Yaser Yacoob, and Dong Yu. Mmc: Advancing multimodal chart understanding with large-scale instruction tuning. *arXiv preprint arXiv:2311.10774*, 2023c.

Haotian Liu, Chunyuan Li, Yuheng Li, and Yong Jae Lee. Improved baselines with visual instruction tuning. *arXiv: 2310.03744*, 2023d.

Haotian Liu, Chunyuan Li, Qingyang Wu, and Yong Jae Lee. Visual instruction tuning. In *NeurIPS*, 2023e.

Haotian Liu, Chunyuan Li, Yuheng Li, Bo Li, Yuanhan Zhang, Sheng Shen, and Yong Jae Lee. Llava-next: Improved reasoning, ocr, and world knowledge, 2024. URL https://llava-vl.github.io/blog/2024-01-30-llava-next/.

Yuan Liu, Haodong Duan, Yuanhan Zhang, Bo Li, Songyang Zhang, Wangbo Zhao, Yike Yuan, Jiaqi Wang, Conghui He, Ziwei Liu, Kai Chen, and Dahua Lin. Mmbench: Is your multi-modal model an all-around player? *arXiv: 2307.06281*, 2023f.

Yuliang Liu, Zhang Li, Hongliang Li, Wenwen Yu, Mingxin Huang, Dezhi Peng, Mingyu Liu, Mingrui Chen, Chunyuan Li, Lianwen Jin, et al. On the hidden mystery of ocr in large multimodal models. *arXiv preprint arXiv:2305.07895*, 2023g.

LMDeployContributors. Lmdeploy: A toolkit for compressing, deploying, and serving llm. https://github.com/InternLM/lmdeploy, 2023.

Haoyu Lu, Wen Liu, Bo Zhang, Bingxuan Wang, Kai Dong, Bo Liu, Jingxiang Sun, Tongzheng Ren, Zhuoshu Li, Yaofeng Sun, et al. Deepseek-vl: Towards real-world vision-language understanding. *arXiv preprint arXiv:2403.05525*, 2024.

Pan Lu, Ran Gong, Shibiao Jiang, Liang Qiu, Siyuan Huang, Xiaodan Liang, and Song-Chun Zhu. Inter-gps: Interpretable geometry problem solving with formal language and symbolic reasoning. *arXiv preprint arXiv:2105.04165*, 2021.

Pan Lu, Swaroop Mishra, Tony Xia, Liang Qiu, Kai-Wei Chang, Song-Chun Zhu, Oyvind Tafjord, Peter Clark, and Ashwin Kalyan. Learn to explain: Multimodal reasoning via thought chains for science question answering. In *NeurIPS*, 2022a.

Pan Lu, Liang Qiu, Kai-Wei Chang, Ying Nian Wu, Song-Chun Zhu, Tanmay Rajpurohit, Peter Clark, and Ashwin Kalyan. Dynamic prompt learning via policy gradient for semi-structured mathematical reasoning. *arXiv preprint arXiv:2209.14610*, 2022b.

Pan Lu, Hritik Bansal, Tony Xia, Jiacheng Liu, Chunyuan Li, Hannaneh Hajishirzi, Hao Cheng, Kai-Wei Chang, Michel Galley, and Jianfeng Gao. Mathvista: Evaluating mathematical reasoning of foundation models in visual contexts. *arXiv: 2310.02255*, 2023.

Junhua Mao, Jonathan Huang, Alexander Toshev, Oana Camburu, Alan L. Yuille, and Kevin Murphy. Generation and comprehension of unambiguous object descriptions. In *CVPR*, pp. 11–20, 2016.

Kenneth Marino, Mohammad Rastegari, Ali Farhadi, and Roozbeh Mottaghi. Ok-vqa: A visual question answering benchmark requiring external knowledge. In *CVPR*, pp. 3195–3204, 2019.

Ahmed Masry, Xuan Long Do, Jia Qing Tan, Shafiq Joty, and Enamul Hoque. Chartqa: A benchmark for question answering about charts with visual and logical reasoning. In *ACL*, pp. 2263–2279, 2022.

Minesh Mathew, Viraj Bagal, Rubèn Tito, Dimosthenis Karatzas, Ernest Valveny, and CV Jawahar. Infographicvqa. In *WACV*, pp. 1697–1706, 2022.

Brandon McKinzie, Zhe Gan, Jean-Philippe Fauconnier, Sam Dodge, Bowen Zhang, Philipp Dufter, Dhruti Shah, Xianzhi Du, Futang Peng, Floris Weers, Anton Belyi, Haotian Zhang, Karanjeet Singh, Doug Kang, Ankur Jain, Hongyu Hè, Max Schwarzer, Tom Gunter, Xiang Kong, Aonan Zhang, Jianyu Wang, Chong Wang, Nan Du, Tao Lei, Sam Wiseman, Guoli Yin, Mark Lee, Zirui Wang, Ruoming Pang, Peter Grasch, Alexander Toshev, and Yinfei Yang. MM1: methods, analysis & insights from multimodal LLM pre-training. *arXiv: 2403.09611*, 2024.

Nitesh Methani, Pritha Ganguly, Mitesh M Khapra, and Pratyush Kumar. Plotqa: Reasoning over scientific plots. In *WACV*, pp. 1527–1536, 2020.

Anand Mishra, Shashank Shekhar, Ajeet Kumar Singh, and Anirban Chakraborty. Ocr-vqa: Visual question answering by reading text in images. In *ICDAR*, pp. 947–952, 2019.

OpenAI. GPT-4 technical report. *arXiv: 2303.08774*, 2023.

Zhiliang Peng, Wenhui Wang, Li Dong, Yaru Hao, Shaohan Huang, Shuming Ma, and Furu Wei. Kosmos-2: Grounding multimodal large language models to the world. *arXiv preprint arXiv:2306.14824*, 2023.

Alec Radford, Jong Wook Kim, Chris Hallacy, Aditya Ramesh, Gabriel Goh, Sandhini Agarwal, Girish Sastry, Amanda Askell, Pamela Mishkin, Jack Clark, Gretchen Krueger, and Ilya Sutskever. Learning transferable visual models from natural language supervision. In *ICML*, volume 139, pp. 8748–8763, 2021.

David Raposo, Sam Ritter, Blake Richards, Timothy Lillicrap, Peter Conway Humphreys, and Adam Santoro. Mixture-of-depths: Dynamically allocating compute in transformer-based language models. *arXiv preprint arXiv:2404.02258*, 2024.

Anna Rohrbach, Atousa Torabi, Marcus Rohrbach, Niket Tandon, Chris Pal, Hugo Larochelle, Aaron Courville, and Bernt Schiele. Movie description. *International Journal of Computer Vision*, 2017. URL http://link.springer.com/article/10.1007/s11263-016-0987-1?wt_mc=Internal.Event.1.SEM.ArticleAuthorOnlineFirst.

Christoph Schuhmann, Romain Beaumont, Richard Vencu, Cade Gordon, Ross Wightman, Mehdi Cherti, Theo Coombes, Aarush Katta, Clayton Mullis, Mitchell Wortsman, et al. Laion-5b: An open large-scale dataset for training next generation image-text models. *NeurIPS*, 35:25278–25294, 2022a.

Christoph Schuhmann, Andreas Köpf, Richard Vencu, Theo Coombes, and Romain Beaumont. Laion coco: 600m synthetic captions from laion2b-en. *https://laion.ai/blog/laion-coco/*, 2022b.

Dustin Schwenk, Apoorv Khandelwal, Christopher Clark, Kenneth Marino, and Roozbeh Mottaghi. A-okvqa: A benchmark for visual question answering using world knowledge. In *ECCV*, pp. 146–162, 2022.

Sanket Shah, Anand Mishra, Naganand Yadati, and Partha Pratim Talukdar. Kvqa: Knowledge-aware visual question answering. In *AAAI*, volume 33, pp. 8876–8884, 2019.

Amir Shahroudy, Jun Liu, Tian-Tsong Ng, and Gang Wang. Ntu rgb+ d: A large scale dataset for 3d human activity analysis. In *Proceedings of the IEEE conference on computer vision and pattern recognition*, pp. 1010–1019, 2016.

Shuai Shao, Zeming Li, Tianyuan Zhang, Chao Peng, Gang Yu, Xiangyu Zhang, Jing Li, and Jian Sun. Objects365: A large-scale, high-quality dataset for object detection. In *ICCV*, pp. 8430–8439, 2019.

Sheng Shen, Zhewei Yao, Chunyuan Li, Trevor Darrell, Kurt Keutzer, and Yuxiong He. Scaling vision-language models with sparse mixture of experts. *arXiv preprint arXiv:2303.07226*, 2023.

Baoguang Shi, Cong Yao, Minghui Liao, Mingkun Yang, Pei Xu, Linyan Cui, Serge Belongie, Shijian Lu, and Xiang Bai. Icdar2017 competition on reading chinese text in the wild (rctw-17). In *ICDAR*, volume 1, pp. 1429–1434, 2017.

Oleksii Sidorov, Ronghang Hu, Marcus Rohrbach, and Amanpreet Singh. Textcaps: A dataset for image captioning with reading comprehension. In *ECCV*, volume 12347, pp. 742–758, 2020.

Amanpreet Singh, Vivek Natarajan, Meet Shah, Yu Jiang, Xinlei Chen, Dhruv Batra, Devi Parikh, and Marcus Rohrbach. Towards VQA models that can read. In *CVPR*, 2019.

Amanpreet Singh, Guan Pang, Mandy Toh, Jing Huang, Wojciech Galuba, and Tal Hassner. Textocr: Towards large-scale end-to-end reasoning for arbitrary-shaped scene text. In *CVPR*, pp. 8802–8812, 2021.

Yipeng Sun, Zihan Ni, Chee-Kheng Chng, Yuliang Liu, Canjie Luo, Chun Chet Ng, Junyu Han, Errui Ding, Jingtuo Liu, Dimosthenis Karatzas, et al. Icdar 2019 competition on large-scale street view text with partial labeling-rrc-lsvt. In *ICDAR*, pp. 1557–1562, 2019.

Rohan Taori, Ishaan Gulrajani, Tianyi Zhang, Yann Dubois, Xuechen Li, Carlos Guestrin, Percy Liang, and Tatsunori B Hashimoto. Alpaca: A strong, replicable instruction-following model. *Stanford Center for Research on Foundation Models. https://crfm. stanford. edu/2023/03/13/alpaca. html*, 3(6):7, 2023.

Gemini Team, Rohan Anil, Sebastian Borgeaud, Yonghui Wu, Jean-Baptiste Alayrac, Jiahui Yu, Radu Soricut, Johan Schalkwyk, Andrew M Dai, Anja Hauth, et al. Gemini: a family of highly capable multimodal models. *arXiv: 2312.11805*, 2023.

InternLM Team. Internlm: A multilingual language model with progressively enhanced capabilities. https://github.com/InternLM/InternLM, 2023.

Teknium. Openhermes 2.5: An open dataset of synthetic data for generalist llm assistants. https://huggingface.co/datasets/teknium/OpenHermes-2.5, 2023.

Hugo Touvron, Thibaut Lavril, Gautier Izacard, Xavier Martinet, Marie-Anne Lachaux, Timothée Lacroix, Baptiste Rozière, Naman Goyal, Eric Hambro, Faisal Azhar, Aurélien Rodriguez, Armand Joulin, Edouard Grave, and Guillaume Lample. Llama: Open and efficient foundation language models. *arXiv: 2302.13971*, 2023a.

Hugo Touvron, Louis Martin, Kevin Stone, Peter Albert, Amjad Almahairi, Yasmine Babaei, Nikolay Bashlykov, Soumya Batra, Prajjwal Bhargava, Shruti Bhosale, et al. Llama 2: Open foundation and fine-tuned chat models. *arXiv: 2307.09288*, 2023b.

Ashish Vaswani, Noam Shazeer, Niki Parmar, Jakob Uszkoreit, Llion Jones, Aidan N. Gomez, Lukasz Kaiser, and Illia Polosukhin. Attention is all you need. In *NIPS*, pp. 5998–6008, 2017.

Andreas Veit, Tomas Matera, Lukas Neumann, Jiri Matas, and Serge Belongie. Coco-text: Dataset and benchmark for text detection and recognition in natural images. *arXiv preprint arXiv:1601.07140*, 2016.

Junke Wang, Lingchen Meng, Zejia Weng, Bo He, Zuxuan Wu, and Yu-Gang Jiang. To see is to believe: Prompting gpt-4v for better visual instruction tuning. *arXiv preprint arXiv:2311.07574*, 2023.

Weiyun Wang, Min Shi, Qingyun Li, Wenhai Wang, Zhenhang Huang, Linjie Xing, Zhe Chen, Hao Li, Xizhou Zhu, Zhiguo Cao, et al. The all-seeing project: Towards panoptic visual recognition and understanding of the open world. In *ICLR*, 2024a.

Wenhui Wang, Hangbo Bao, Li Dong, Johan Bjorck, Zhiliang Peng, Qiang Liu, Kriti Aggarwal, Owais Khan Mohammed, Saksham Singhal, Subhojit Som, and Furu Wei. Image as a foreign language: Beit pretraining for all vision and vision-language tasks. *arXiv: 2208.10442*, 2022.

Xinlong Wang, Xiaosong Zhang, Zhengxiong Luo, Quan Sun, Yufeng Cui, Jinsheng Wang, Fan Zhang, Yueze Wang, Zhen Li, Qiying Yu, Yingli Zhao, Yulong Ao, Xuebin Min, Tao Li, Boya Wu, Bo Zhao, Bowen Zhang, Liangdong Wang, Guang Liu, Zheqi He, Xi Yang, Jingjing Liu, Yonghua Lin, Tiejun Huang, and Zhongyuan Wang. Emu3: Next-token prediction is all you need. *arXiv: 2409.18869*, 2024b.

Xiyao Wang, Yuhang Zhou, Xiaoyu Liu, Hongjin Lu, Yuancheng Xu, Feihong He, Jaehong Yoon, Taixi Lu, Gedas Bertasius, Mohit Bansal, et al. Mementos: A comprehensive benchmark for multimodal large language model reasoning over image sequences. *arXiv preprint arXiv:2401.10529*, 2024c.

Bo Wu, Shoubin Yu, Zhenfang Chen, Joshua B Tenenbaum, and Chuang Gan. Star: A benchmark for situated reasoning in real-world videos. In *Thirty-fifth Conference on Neural Information Processing Systems (NeurIPS)*, 2021.

Jinheng Xie, Weijia Mao, Zechen Bai, David Junhao Zhang, Weihao Wang, Kevin Qinghong Lin, Yuchao Gu, Zhijie Chen, Zhenheng Yang, and Mike Zheng Shou. Show-o: One single transformer to unify multimodal understanding and generation. *arXiv preprint arXiv:2408.12528*, 2024.

Zhengyuan Yang, Linjie Li, Kevin Lin, Jianfeng Wang, Chung-Ching Lin, Zicheng Liu, and Lijuan Wang. The dawn of lmms: Preliminary explorations with gpt-4v (ision). *arXiv: 2309.17421*, 9, 2023.

Yuan Yao, Tianyu Yu, Ao Zhang, Chongyi Wang, Junbo Cui, Hongji Zhu, Tianchi Cai, Haoyu Li, Weilin Zhao, Zhihui He, et al. Minicpm-v: A gpt-4v level mllm on your phone. *arXiv preprint arXiv:2408.01800*, 2024.

Peter Young, Alice Lai, Micah Hodosh, and Julia Hockenmaier. From image descriptions to visual denotations: New similarity metrics for semantic inference over event descriptions. *TACL*, 2: 67–78, 2014.

Licheng Yu, Patrick Poirson, Shan Yang, Alexander C. Berg, and Tamara L. Berg. Modeling context in referring expressions. In *ECCV*, volume 9906, pp. 69–85, 2016.

Longhui Yu, Weisen Jiang, Han Shi, Jincheng Yu, Zhengying Liu, Yu Zhang, James T Kwok, Zhenguo Li, Adrian Weller, and Weiyang Liu. Metamath: Bootstrap your own mathematical questions for large language models. *arXiv preprint arXiv:2309.12284*, 2023a.

Weihao Yu, Zhengyuan Yang, Linjie Li, Jianfeng Wang, Kevin Lin, Zicheng Liu, Xinchao Wang, and Lijuan Wang. Mm-vet: Evaluating large multimodal models for integrated capabilities. *arXiv: 2308.02490*, 2023b.

Tai-Ling Yuan, Zhe Zhu, Kun Xu, Cheng-Jun Li, Tai-Jiang Mu, and Shi-Min Hu. A large chinese text dataset in the wild. *Journal of Computer Science and Technology*, 34:509–521, 2019.

Xiang Yue, Yuansheng Ni, Kai Zhang, Tianyu Zheng, Ruoqi Liu, Ge Zhang, Samuel Stevens, Dongfu Jiang, Weiming Ren, Yuxuan Sun, et al. Mmmu: A massive multi-discipline multimodal understanding and reasoning benchmark for expert agi. *arXiv: 2311.16502*, 2023.

Seniha Esen Yuksel, Joseph N Wilson, and Paul D Gader. Twenty years of mixture of experts. *IEEE transactions on neural networks and learning systems*, 23(8):1177–1193, 2012.

Yuexiang Zhai, Shengbang Tong, Xiao Li, Mu Cai, Qing Qu, Yong Jae Lee, and Yi Ma. Investigating the catastrophic forgetting in multimodal large language models. *arXiv preprint arXiv:2309.10313*, 2023.

Biao Zhang and Rico Sennrich. Root mean square layer normalization. *Advances in Neural Information Processing Systems*, 32, 2019.

Rui Zhang, Yongsheng Zhou, Qianyi Jiang, Qi Song, Nan Li, Kai Zhou, Lei Wang, Dong Wang, Minghui Liao, Mingkun Yang, et al. Icdar 2019 robust reading challenge on reading chinese text on signboard. In *ICDAR*, pp. 1577–1581, 2019.

Bo Zhao, Boya Wu, and Tiejun Huang. SVIT: scaling up visual instruction tuning. *arXiv: 2307.04087*, 2023.

Lianmin Zheng, Wei-Lin Chiang, Ying Sheng, Siyuan Zhuang, Zhanghao Wu, Yonghao Zhuang, Zi Lin, Zhuohan Li, Dacheng Li, Eric Xing, et al. Judging llm-as-a-judge with mt-bench and chatbot arena. *NeurIPS*, 36, 2024.

Chunting Zhou, Lili Yu, Arun Babu, Kushal Tirumala, Michihiro Yasunaga, Leonid Shamis, Jacob Kahn, Xuezhe Ma, Luke Zettlemoyer, and Omer Levy. Transfusion: Predict the next token and diffuse images with one multi-modal model. *arXiv preprint arXiv:2408.11039*, 2024.

A APPENDIX

A.1 MORE DATASET DETAILS

Table 7: **Summary of datasets used in instruction tuning.**

Task	Dataset
Captioning	TextCaps (en) (Sidorov et al., 2020), ShareGPT-4o (en&zh) (Chen et al., 2024c)
General QA	VQAv2 (en) (Goyal et al., 2017), GQA (en) (Hudson & Manning, 2019), OKVQA (en) (Marino et al., 2019), VSR (en) (Liu et al., 2023a), VisualDialog (en) (Das et al., 2017)
Science	AI2D (en) (Kembhavi et al., 2016), ScienceQA (en) (Lu et al., 2022a), TQA (en) (Kembhavi et al., 2017)
Chart	ChartQA (en) (Masry et al., 2022), MMC-Inst (en) (Liu et al., 2023c), DVQA (en) (Kafle et al., 2018), PlotQA (en) (Methani et al., 2020), LRV-Instruction (en) (Liu et al., 2023b)
Mathematics	GeoQA+ (en) (Cao & Xiao, 2022), TabMWP (en) (Lu et al., 2022b), MathQA (en) (Yu et al., 2023a), CLEVR-Math/Super (en) (Lindström & Abraham, 2022; Li et al., 2023c), Geometry3K (en) (Lu et al., 2021)
Knowledge	KVQA (en) (Shah et al., 2019), A-OKVQA (en) (Schwenk et al., 2022), ViQuAE (en) (Lerner et al., 2022), Wikipedia (en&zh) (He et al., 2023)
OCR	OCRVQA (en) (Mishra et al., 2019), InfoVQA (en) (Mathew et al., 2022), TextVQA (en) (Singh et al., 2019), ArT (en&zh) (Chng et al., 2019), COCO-Text (en) (Veit et al., 2016), CTW (zh) (Yuan et al., 2019), LSVT (zh) (Sun et al., 2019), RCTW-17 (zh) (Shi et al., 2017), ReCTs (zh) (Zhang et al., 2019), SynthDoG (en&zh) (Kim et al., 2022), ST-VQA (en) (Biten et al., 2019)
Document	DocVQA (en) (Clark & Gardner, 2018), Common Crawl PDF (en&zh)
Grounding	RefCOCO/+/g (en) (Yu et al., 2016; Mao et al., 2016), Visual Genome (en) (Krishna et al., 2017)
Conversation	LLaVA-150K (en&zh) (Liu et al., 2023e), LVIS-Instruct4V (en) (Wang et al., 2023), ALLaVA (en&zh) (Chen et al., 2024a), Laion-GPT4V (en) (LAION, 2023), ShareGPT (en&zh) (Zheng et al., 2024), SVIT (en&zh) (Zhao et al., 2023)
Text-only	OpenHermes2.5 (en) (Teknium, 2023), Alpaca-GPT4 (en) (Taori et al., 2023), COIG-CQIA (zh) (Bai et al., 2024), ShareGPT (en&zh) (Zheng et al., 2024)
Video	EgoTaskQA (en) (Jia et al., 2022), Mementos (en) (Wang et al., 2024c), STAR (en) (Wu et al., 2021), NTU RGB+D (en) (Shahroudy et al., 2016), VideoChat2IT (en&zh) (Li et al., 2023b), LSMDC-QA (en) (Rohrbach et al., 2017), ShareGPT-4o (en&zh) (Chen et al., 2024c)
Handwritten	SROIE (en) (Huang et al., 2019), FUNSD (en) (Guillaume Jaume, 2019), POIE (en) (Kuang et al., 2023)

The datasets used in the instruction fine-tuning stage are listed in Tab. 7.

A.2 MORE TRAINING DETAILS

Table 8: **Hyper-parameters used in the pre-training and instruction tuning of Mono-InternVL.**

Configuration	Concept Learning (S1.1)	Semantic Learning (S1.2)	Alignment Learning (S1.3)	Instruction Tuning (S2)
Maximum numer of patches	$1,280$	$1,792$	$3,328$	$6,400$
LLM sequence length	$1,425$	$1,925$	$4,096$	$8,192$
Use thumbnail		✓		
Optimizer		AdamW		
Optimizer hyperparameters		$\beta_1 = 0.9, \beta_2 = 0.999, eps = 1e^{-8}$		
Peak learning rate	$1e^{-4}$	$1e^{-4}$	$5e^{-5}$	$2e^{-5}$
Learning rate schedule	constant with warm-up	constant with warm-up	cosine decay	cosine decay
Drop path rate		0.1		
Weight decay		0.01		
Training steps	450k	126k	70k	14k
Warm-up steps	100	100	100	420
Global batch size	$2,048$	$2,048$	$2,048$	$1,024$
Gradient accumulation	1	1	1	4
Numerical precision		`bfloat16`		

Hyper-parameters used in the training stages are listed in Tab. 8.

A.3   MORE ABLATION STUDIES

In Fig. 6, we provide the full results of Fig. 4 with all the downstream tasks.
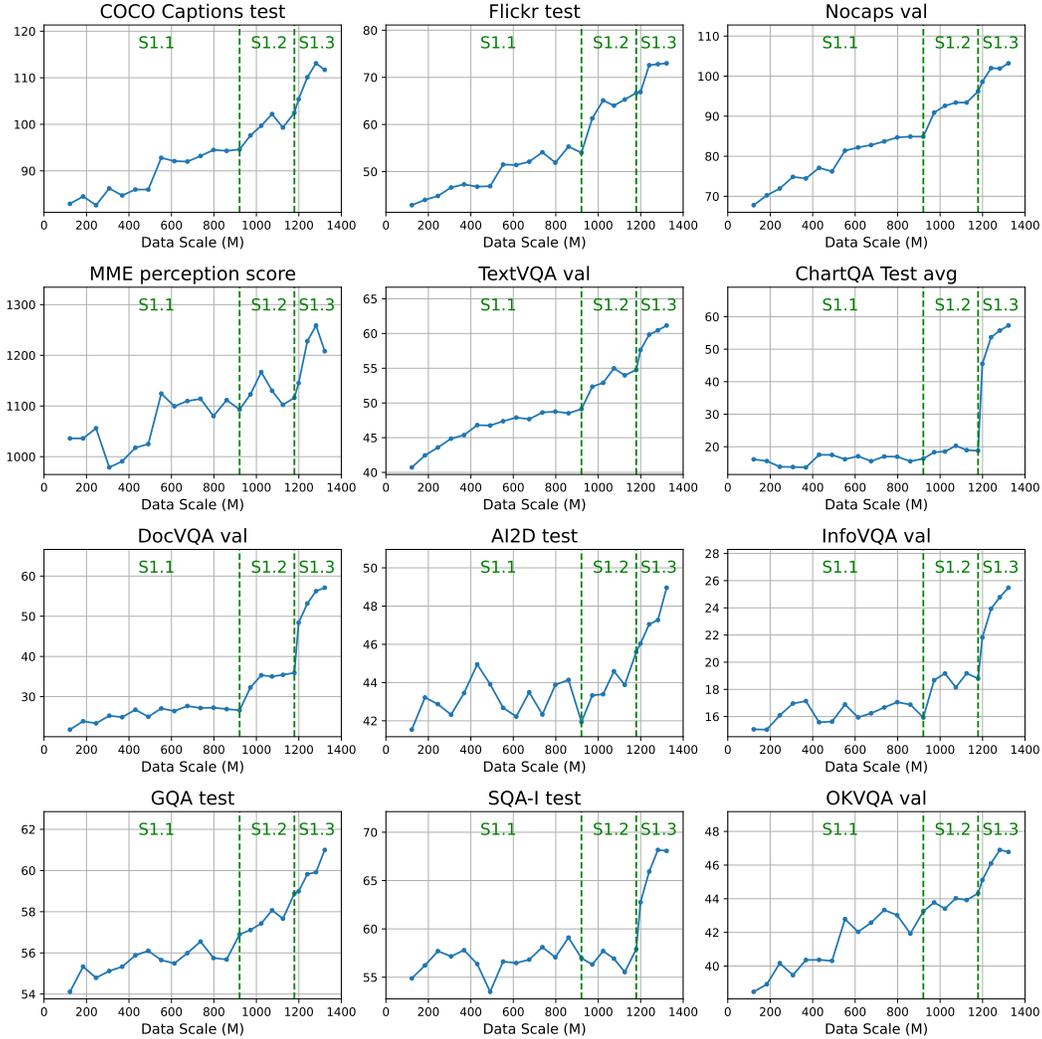

Figure 6: **Complete results of downstream performance breakdown with the increase of pre-training data size.**

In Tab. 9, we examine the effects of freezing and unfreezing attention layers in alignment learning. We observe that unfreezing attention results in consistent improvements across all metrics, suggesting that it is crucial to optimize the multi-head attentions in this sub-stage for better vision-language alignment.

Table 9: **Results of freezing and unfreezing attention in alignment learning.** "T-Param" refers to trainable parameters. All models are pre-trained on 20 millions of data in alignment learning and fine-tuned on instruction data from LLaVA-665k (Liu et al., 2023d).

Methods	#T-Param	MME-P	DocVQA	InfoVQA	SQA-I	GQA	ChartQA	AI2D
Freeze attention	1.8B	1136	39.5	19.7	56.5	59.1	27.2	44.1
Unfreeze attention	3.0B	1153	49.3	22.7	61.8	59.9	49.5	46.4

A.4 VISUALIZATIONS

Image captioning and OCR
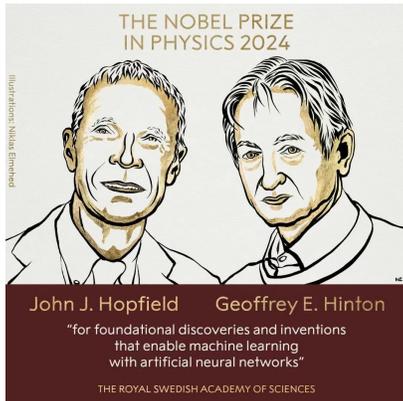
Prompt: What is the content in this picture?

Response: The image is a graphical representation, primarily informational in nature. It features two individuals depicted in line art style. The background of the image is lightcolored.

At the top of the image, there's text that reads "THE NOBEL PRIZE IN PHYSICS 2024." This indicates that the award being discussed in this image pertains to physics and is scheduled for the year 2024.

Below this header, there are two names mentioned: John J. Hopfield and Geoffrey E. Hinton. Further down, there is a quote attributed to both named individuals: "for foundational discoveries and inventions that enable machine learning with artificial neural networks." This quote suggests that both John J. Hopfield and Geoffrey E. Hinton made significant contributions to the field of artificial intelligence and neural networks, which may have involved pioneering discoveries and innovations that were crucial for developing machine learning technologies.

Finally, at the bottom, there's another text stating: "THE ROYAL SWEDISH ACADEMY OF SCIENCES." This indicates that John J. Hopfield and Geoffrey E. Hinton have been recognized by the Royal Swedish Academy of Sciences.

Overall, this image appears to serve as a tribute or recognition of the achievements of these scientists in the field of physics, particularly relating to artificial intelligence and neural networks.

Prompt: Describe this image.

Response: This image depicts a bustling urban scene at night in an animation style, with a large electronic billboard prominently displaying the words "YUNIKA VISION" in bright white letters against a black background. The billboard is surrounded by several other tall buildings, including those of well-known companies such as HITACHI, TOSHIBA, SHARP, SONY, PANASONIC, and NEC.

In the foreground, there are multiple train tracks that intersect near what appears to be an elevated railway or subway system. Several trains are visible, indicating active transportation amidst the busy cityscape.

The skyline is dotted with various other commercial and residential structures, contributing to the sense of a thriving metropolis. Trees can also be seen around the area, providing some greenery amidst the urban environment. Overall, the image captures the dynamic energy of a modern city at night, with its blend of technology, commerce, and human activity.

Visual grounding

Prompt: Detect the <ref>the American Shorthair</ref> in the image with its bounding box.

Response: <ref> the American Shorthair </ref> <box> [[229, 125, 660, 932]] </box>
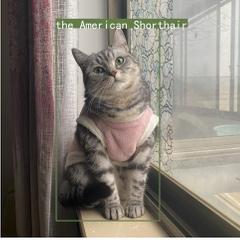
Prompt: Please describe the detected object.

Response: The object in the image is a cat. The cat has gray fur with black stripes and is wearing a pink sweater. It appears to be sitting on a windowsill, looking up attentively towards the camera.

Prompt: Detect the <ref>the tallest building</ref> in the image with its bounding box.

Response: <ref> the tallest building </ref> <box> [[529, 313, 580, 591]] </box>

Prompt: Please infer where this place is.

Response: This image depicts a stunning view of the skyline of Shanghai, China. The prominent features in the skyline include several high-rise buildings with unique structures such as the Oriental Pearl Tower and the Shanghai World Financial Center. There is also a distinctive arch bridge spanning across a river, which appears to be part of Shanghai's famous Huangpu River waterfront area known for its historic sites and modern development.

VQA

Prompt: Describe the image.

Response: The image features a large adult dog lying on its side, likely the mother of several puppies. The adult dog has brown and white fur with distinct markings on its face. She is surrounded by several small puppies, all of which are nursing from her body or resting on a light blue towel that covers part of the floor. The setting appears to be indoors, possibly in a home environment given the tiled flooring and the soft, comfortable-looking towel. The atmosphere seems calm and nurturing as the dogs interact closely together.

Prompt: Please tell me the exact number of golden retrievers in the picture.

Response: There are a total of six golden retrievers in the picture.

Chinese OCR

> 你知道吗。晚上和早上的风
> 开始冷了．树叶也开始落了
> 下次见面就该穿长袖了
> 对了．好久不见．
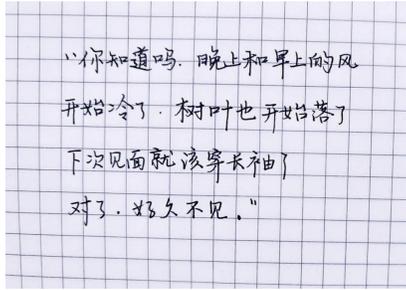
Prompt: 识别图中文字。

Response: 图中文字如下：
"你知道吗。晚上和早上的风 开始冷了，树叶也开始落了 下次见面就该穿长袖了 对了。好久不见。"

Code generation

$$\mathcal{L}_{self\text{-}dist}(G_{AB}, p_A) = \mathbb{E}_{\mathbf{x}\sim p_A}|\frac{1}{\sigma_A}(\|L(\mathbf{x}) - R(\mathbf{x})\|_1 - \mu_A)$$
$$-\frac{1}{\sigma_B}(\|G_{AB}(L(\mathbf{x})) - G_{AB}(R(\mathbf{x}))\|_1 - \mu_B)|$$

Prompt: Convert the formula in the figure to latex format.

Response: Certainly! Here is the formula from the figure in LaTeX format:

```
\begin{equation}
\begin{aligned}
    \mathcal{L}_{self-dist}(G_{AB}, p_A) = \mathbb{E}_{\textbf{x}\sim p_A}|
    \frac{1}{\sigma_A}(|| L(\textbf{x}) - R(\textbf{x}) ||_1 - \mu_A)\\
    - \frac{1}{\sigma_B}(||G_{AB}(L(\textbf{x})) - G_{AB}(R(\textbf{x}))||_1 - \mu_B)|
\end{aligned}
\end{equation}
```

Document understanding
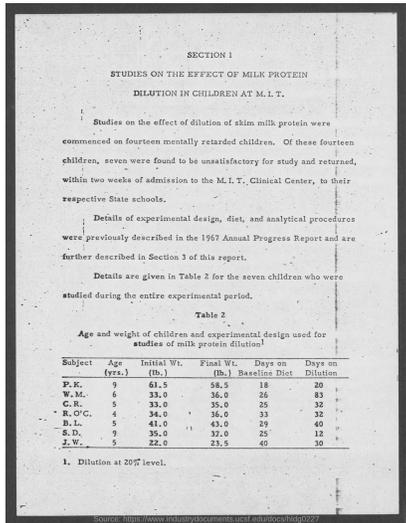
Prompt: What is the age of subject B.L.?

Response: B.L. is 5 years old at the time of study on the effect of milk protein dilution.

Prompt: Whose initial weight is the largest? What is it?

Response: The largest initial weight in the table is for P.K. with 61.5 pounds (lb.).

Prompt: How many children participated in the experiment in total?

Response: There are a total of 14 children who participated in the experiment.

Math
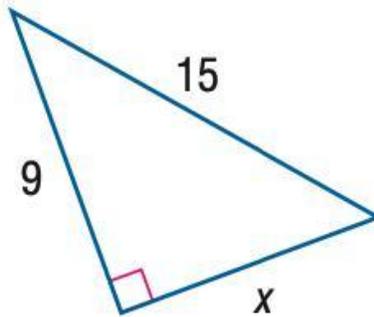
Prompt: The figure shows a right-angled triangle. What is the value of x?

Response: To find the value of x, we can use the Pythagorean theorem, which states: $a^2 + b^2 = c^2$ where c is the hypotenuse (the side opposite the right angle), and a and b are the other two sides.
In this triangle:
The length of the hypotenuse (c) is 15.
One leg (a) is 9.
The other leg (b) is x.
Using the Pythagorean theorem:
$9^2 + x^2 = 15^2$
$81 + x^2 = 225$
Now, solve for x:
$x^2 = 225 - 81$
$x^2 = 144$
$x = \sqrt{144}$
$x = 12$
So, the value of x is 12.